

Али Дж. Давуд Аль-Хафаджи, Г.С. Панатов, А.С. Болдырев

ОПТИМИЗАЦИЯ АЭРОДИНАМИЧЕСКИХ ХАРАКТЕРИСТИК БЕСПИЛОТНОГО ЛЕТАТЕЛЬНОГО АППАРАТА С ИСПОЛЬЗОВАНИЕМ КРЫЛА ПЕРЕМЕННОЙ СТРЕЛОВИДНОСТИ

Беспилотные летательные аппараты (БПЛА) могут иметь различные формы в зависимости от типа и условий полета. В данной работе проведена оптимизация аэродинамических свойств БПЛА за счет угла стреловидности крыла (угла стреловидности) для уменьшения волнового сопротивления и задержки начала дивергенции сопротивления. Для этого использовались модели беспилотных летательных аппаратов (БПЛА), разработанные с пятью различными углами стреловидности крыла (15° , 20° , 25° , 30° и 35°) и различным удлинением с постоянным коэффициентом конусности = 0,2. Каждое крыло было построено с аэродинамическим профилем для корневой и концевой хорд SD8020 с малым числом Маха, равным 0,058 (т. е. скоростью, равной 20 м/с). Все модели крыла были построены для трехмерного изображения с использованием программы SOLIDWORKS, а затем модели для этого крыла были проанализированы с использованием ANSYS FLUENT. Были проведены расчеты значения аэродинамического качества для определения того, какой БПЛА имеет оптимальное значение подъемной силы и наименьшее лобовое сопротивление в зависимости от угла атаки (0° , 2° и 4°). Результаты показывают, что аэродинамические характеристики изменяются в зависимости от величины угла стреловидности и удлинения, максимальное аэродинамическое качество достигается у БПЛА с углом стреловидностью 15° и углом атаки 2° , минимальное аэродинамическое качество у БПЛА со стреловидностью 35° , а угол атаки 0° . Из-за постоянного коэффициента конусности, равного 0,2, площадь крыла у каждой модели разная. Лучшая модель с максимальным отношением подъемной силы к лобовому сопротивлению имеет площадь крыла, равную $1,68 \text{ м}^2$, а модель с минимальным аэродинамическим сопротивлением имеет площадь крыла, равную $0,65 \text{ м}^2$.

Беспилотный летательный аппарат, подъем и перетаскивание, угол поворота, соотношение сторон, SOLIDWORKS, CFD, ANSYS (Fluent).

Ali J. Dawood Al-Khafaji, G.S. Panatov, A.S. Boldyrev

UNMANNED AERIAL VEHICLE AERODYNAMICS PERFORMANCE OPTIMIZATION USING VARIABLE SWEEP WING ANGLE

The unmanned aerial vehicles (UAVs) can take many forms depending on the type of UAV duty and condition of flight. In this project, optimization of UAVs aerodynamics property through the sweep angle of wing (sweepback angle) to reduce wave drag and delay the onset of drag divergence. therefor models of unmanned aerial vehicles (UAVs) designed with five different sweepback wing angle (15° , 20° , 25° , 30° , and 35°) and different aspect ratio with constant taper ratio = 0.2 have been used. Every wing was built with airfoil for root and tip chord SD8020, with low Mach number equal to 0.058 (i.e., Velocity equal to 20 m/s). The whole models of a wing were plotted for a three-dimensional using the SOLIDWORKS software program, and then the models of this wing were analyzed employing ANSYS FLUENT. Calculations of the value of lift to drag ratio were made for deciding which UAV has optimum value of lift and the lowest drag versus the attack angle (0° , 2° , and 4°). The results Show that the aerodynamics performance changes according to the value of the sweepback angle and aspect ratio, the maximum lift to drag ratio achieved at UAV with sweepback angle 15° and the angle of attack is 2° , minimum lift to drag ratio at UAV with sweepback angle 35° and the angle of attack is 0° . Due to constant taper ratio which equal to 0.2 the wing area different according to each model. Best model with maximum lift to drag ratio has wing area equal to 1.68 м^2 while model with minimum lift to drag has wing area equal to 0.65 м^2 .

UAV; lift and drag; sweepback angle; aspect ratio; SOLIDWORKS; CFD; ANSYS (Fluent).

1. Introduction. During the aircraft design process, an aircraft designer faces several of the challenges. Designing an efficient wing that meets the established standards is one of the most significant responsibilities. This is usually feasible due to the wing's various geometrical and aerodynamic properties being optimized [1]. Presently, aviation concentrates on cost-effective, fuel-efficient, long-range systems with minimal operational expenses. The increased need for airborne activities has led to the introduction of unmanned aircraft that can stay in the air for far longer periods of time than planes with pilots. To achieve these goals, the UAV design has been substantially explored. At the moment, UAVs can last for more than a day [2]. The term "unmanned aerial vehicle" (UAV) refers to a vehicle that may operate remotely, semi-autonomously, or fully autonomously without the need for a pilot. In comparison to piloted aerial photogrammetry, it is a current and low-cost application. UAVs come in a variety of kinds, classifications, and categories [3]. The size categories for unmanned aerial vehicles (UAVs) range from nano air vehicles (NAVs) with a wing span of under 4 cm to high altitude long endurance (HALE) aircraft with a wing span of 35 meters or more. Micro (MAV), mini, close-range, medium range or tactical, and medium altitude long endurance are some of the classifications of UAVs in between [4]. For decades, the aviation industry has been fascinated by the development of unmanned aerial vehicles (UAVs). In the conceptual design of an airplane, aerodynamic design is extremely important. The structure and systems of an aircraft, as well as the manufacturing process, are heavily influenced by the aerodynamic design layout. A good aerodynamic design allows an airplane to operate well while also lowering expenses due to decreased fuel consumption. Many criteria must be decided at the outset of the aircraft's conceptual design. For conventional aircraft, studies have established aircraft conceptual design processes and assessed numerous procedures [5].

A variety of performance characteristics may be used to classify UAVs. Wind loading, speed, range, endurance, and weight are all important characteristics that define different types of UAVs and provide the basis for appropriate classification. Depending on the Strategic, Tactical, UAV Size, and Special Task. According to their maximum gross take-off weight, usual flying altitude, and velocity, the US Department of Defence divided UAVs into five categories: small, medium, big, larger, and largest. The most frequent categories, however, are based on the size, endurance, and structure [6, 7].

2. Wing geometry parameters. A wing is formed of two-dimensional airfoil sections that form a three-dimensional shape. Wings, horizontal tails, vertical tails, canards, and/or other lifting surfaces are produced by arranging the airfoil sections in various spanwise configurations. When introducing the parameters that define the wing planform, it's important to pay attention to the presence of flow components in the spanwise direction (three-dimensional flow). In other words, airfoil section properties deal with two-dimensional flow, whereas wing planform qualities deal with three-dimensional flow. The planform (or projected shape) of a wing is often described using many concepts. The terms that are relevant to characterizing the aerodynamic properties of a wing are shown in Fig. 1 [8]:

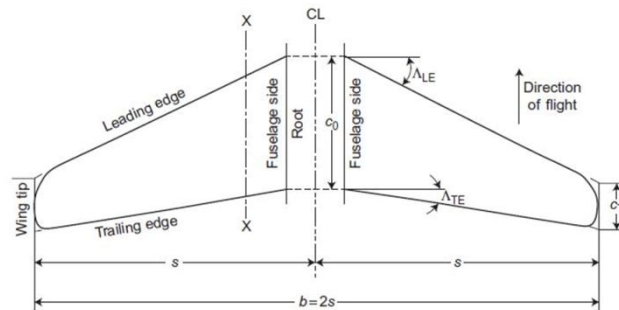


Fig. 1. Geometric characteristics of the wing planform [8]

2.1. Wingspan. The wingspan is defined as the distance between the two wingtips multiplied by the dimension b . The wing semi-span is the distance $b/2$ between each tip and the centreline [9].

2.2. Chords. The tip and root chords are the two lengths C_t and C_r , respectively; under the alternate convention, the root chord is the distance between the intersections of the leading and trailing edges formed with the fuselage centreline. The taper ratio is defined as C_t/C_r . The reciprocal of this, C_r/C_t , is sometimes used as the taper ratio. $C_t/C_r < 1$ for most wings [9].

2.3. Sweepback angle (Λ). The sweepback angle is the angle formed by the aircraft's OY lateral axis and the 25% MAC line (or occasionally the leading edge of the wing). The sweepback angle is denoted by the Greek letter Lambda. Increased sweepback angle has the benefit of lowering the effective thickness/chord ratio of the wing. The physical wing depth stays the same, but the effective wing depth is reduced, resulting in a higher critical Mach number. In contrast, too much sweepback angle can cause aileron reversal, aerodynamic tip stalling, shock stalling, and wing deformation due to partial spanwise flow towards the wingtips [8, 10]. Swept wings are usually associated with high-speed (transonic or supersonic) flight, while zero-sweep wings are occasionally used on high-speed aircraft, and many low-speed aircraft feature swept wings. The second group exists mostly due to stability concerns, particularly in the case of 'flying wing'-type aircraft, which can only be rendered statically stable with nonzero sweep in practice [11].

2.4. Area ratio. The planform area (or projected area) of the wing is simply referred to as the wing area, A . Despite the fact that a fuselage or nacelles may cover a section of the space, the pressure carryover on these surfaces permits reasonable examination of the full planform area [8]. The wing area ratio is calculated by dividing the wing area by the wingspan squared (A/b^2). The reciprocal of aspect ratio is area ratio [10].

$$A = 0.5 * (C_r + C_t) * s. \quad (1)$$

2.5. The aspect ratio (AR). The wing aspect ratio is a key feature that influences both the size and slope of the lift produced drag curve. As a result, it has a direct impact on performance as well as stability and control [1]. The aspect ratio is a measurement of the wing's slenderness or fineness ratio, or the proportions of the wing. It is critical for the aircraft designer to understand the aerodynamic properties of the wing as well as the structural weight analysis. The wing planform has a bigger impact than the wing area. The aspect ratio is defined as the ratio of wingspan to average wing chord (span/chord) or more succinctly (span²/wing area) and is determined by the tip-to-tip wingspan (b) and its chord (c).

$$AR = \frac{b^2}{A} \text{ or } \frac{b}{c} \quad (2)$$

The first ratio (b/c) is applied when calculating rectangular wings; the second ratio (b^2/S) is more efficient when calculating other planform wings. The aspect ratio is small. A high sweepback angle of at least 45° or larger, pointed wingtips, and a straight trailing edge characterize this wing. When opposed to a straight wing, the wing has a larger area per span, resulting in less wing loading and more fuel storage space. Because of its distance from the centre of gravity, the wing is free of flaps, which would be ineffective and operate as elevators, Fig. 2, [8, 10, 11].

For conventional subsonic aircraft and sailplanes, AR, which normally ranges from 6 to 22, has a far larger influence on the generated drag coefficient than the value of the boundary-layer thickness. As a result, the capacity to make the aspect ratio as big as feasible, rather than being near to an elliptical lift distribution, is the major design element for minimizing induced drag. One of Prandtl's lifting-line theory's major wins was the discovery that generated drag coefficient is inversely related to AR [12].

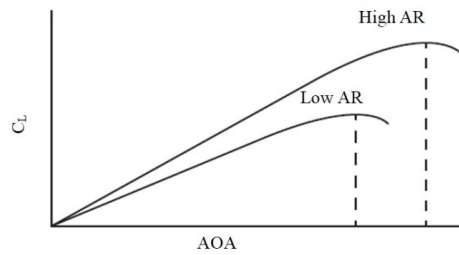


Fig. 2. Aspect Ratio & Lift Coefficient [10]

It's simple to start determining the remaining geometric parameters after the wing area and wingspan have been calculated. Aspect ratio, taper ratio, wing sweep, dihedral, and other features of the wing's geometric arrangement are only a few examples. The geometric arrangement of the wing is comprised of these. The layout has a significant impact on the whole design process, as well as a slew of other aspects of the project. These include, among other things, aerodynamics, performance, stability and control, as well as structural and system layout. The AR, TR, and LE sweeps allow the designer the most control over the wing's aerodynamic properties. This isn't to imply the others aren't significant; they may be thought of as dials for "fine-tuning" the wing design. The AR, TR, and sweep may be determined as a result of a sophisticated optimization; however, this is not always the case. The combined effect of AR and leading edge sweep in Fig. 3 [1].

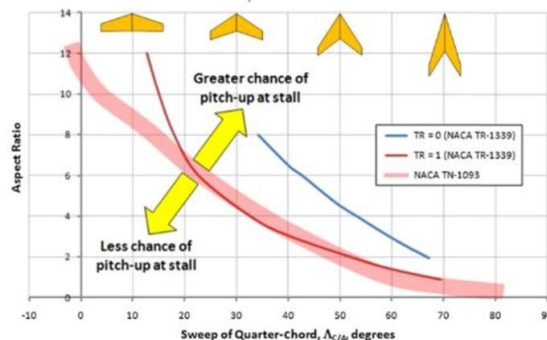


Fig. 3. Empirical pitch-up boundary for a swept-back wing [1]

3. Aerodynamics forces. 3.1. Introduction . For a very long time, aerodynamicists have employed force and moment coefficients to explain the aerodynamics of aircraft. Coefficients are non-dimensional quantities that reflect forces and moments without taking into account the effects of density, velocity, and size. When non-dimensionalizing forces and moments, not all flow properties may be considered. Because of this, even when considering some flight parameters in coefficient form, such as drag, Reynolds number and Mach number remain functions [8]. Thrust, lift, drag, and weight are the main factors that affect an airborne vehicle. The vehicle rotates around the pitch, roll, and yaw axes due to angular moments about those axes. Dynamic pressure, wing area, and dimensionless coefficients are used to calculate lift, drag, and rotational moments. The basic aerodynamic equations that control an air vehicle's performance are the expressions for these quantities [13].

In the context of an aircraft, lift is the amount of force that is directed upward and perpendicular to the direction of flight, or, in the case of an unbroken stream. The phrase "upward" refers to the pilot's head being above the ground. The effect of various atti-

tudes toward flying is depicted in Fig. 4. The vector V depicts the direction of flight, the vector L the lift acting upward, and the vector W the weight of the airplane and the downward vertical.

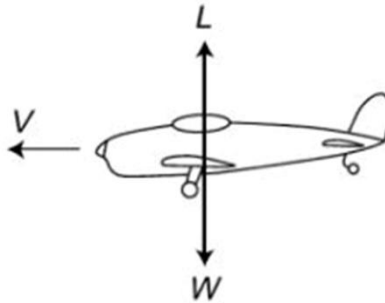


Fig. 4. Direction of the lift force in level flight [14]

Drag is the amount of force operating perpendicular to the path of flight or parallel to the direction of an unbroken stream. It is the force that opposes the aircraft's motion. Regarding its meaning or aim, there is no room for doubt. Therefore, the drag force is constantly in opposition to the lift force. When an airplane is flying horizontally, the moment known as pitching occurs in the plane containing the lift and the drag, or in the vertical plane. When it tends to elevate the aircraft's nose or increase the angle of attack, it is classified as positive [14].

3.2. Aerodynamic Coefficients. These non-dimensional pressure, force, and moment variables have an impact on the flying item. The free stream density ρ and velocity V are employed as characteristic values in non-dimensionalization. The pressure coefficient C_p is calculated using half of the dynamic pressure $\frac{1}{2}\rho V^2$. The wing surface area is taken into account as the typical length, half of the chord length, and as the characteristic area. The sectional lift coefficient C_L , drag coefficient C_D , and moment coefficient C_M , are calculated using the product of dynamic pressure and the half chord, where the square of the half chord is employed. However, the moment coefficient, the drag coefficient, and the coefficient of lift for the finite wing [15].

Lift coefficient

$$C_L = \frac{2L}{\rho S V^2} = \frac{L}{qS}$$

Drag coefficient

$$C_D = \frac{2D}{\rho S V^2} = \frac{D}{qS}$$

Moment coefficient

$$C_M = \frac{M}{qSl}$$

The reference area S and reference length l in the previous coefficients are selected to correspond to the specified geometric body form; for other shapes, S and l may be different things [12, 16–19].

3.3. Angles of attack. The geometric angle of attack is the angle between the relative wind direction and the mean chord of the wing, which is a line drawn between the leading edge and trailing edge of the wing in aeronautics. The orientation in which the wing has no lift is used to calculate the effective angle of attack. To avoid reader confusion, it is important to underline the distinction between the effective angle of attack employed here and the geometric angle of attack used in aeronautics. In Fig. 5, the orientation of a cambered

wing with no geometric angles of attack and the same wing with no effective angles of attack are shown. Since the air is being net-diverted downward, a cambered wing with zero geometric angles of attack has lifted. The same wing has no lift and no net air diversion when the effective angle of attack is zero, according to a definition. The geometric and actual angles of attack are the same in the case of a symmetric wing [20].

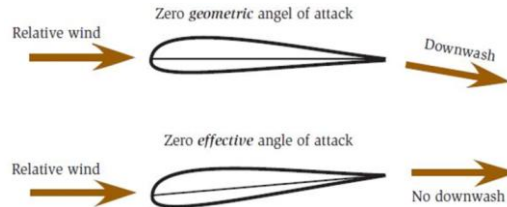


Fig. 5. Definition of geometric and effective angles of attack [20]

4. Model building and analyzing. SOLIDWORKS program was utilized to build four different models which are different in sweep wing angle. Fig. 6 shows the shapes of wings used in this paper with different sweep angle (15°, 20°, 25°, 30°, and 35°). Wing dimensions were used to build these models in 3 dimensions with root chord 1000 mm and tip chord 200 mm, taper ratio constant = 0.2; all models consist of one airfoil (SD8020). Computational Fluid Dynamics (CFD) software/ANSYS (Fluent) was used to analyze the models with assuming that: - enclosure uniform 1 m, mesh - relevance centre – fine, velocity magnitude (m/s) 20, and space three-dimensional time steady viscous SST k-omega. The unmanned aerial vehicles at altitude =3000m, air pressure (68189.15 Pa), (1.31 kg/m³) density, (1.7E-5 kg·m⁻¹·s⁻¹) dynamic viscosity, and (- 4.5 C°) temperature.

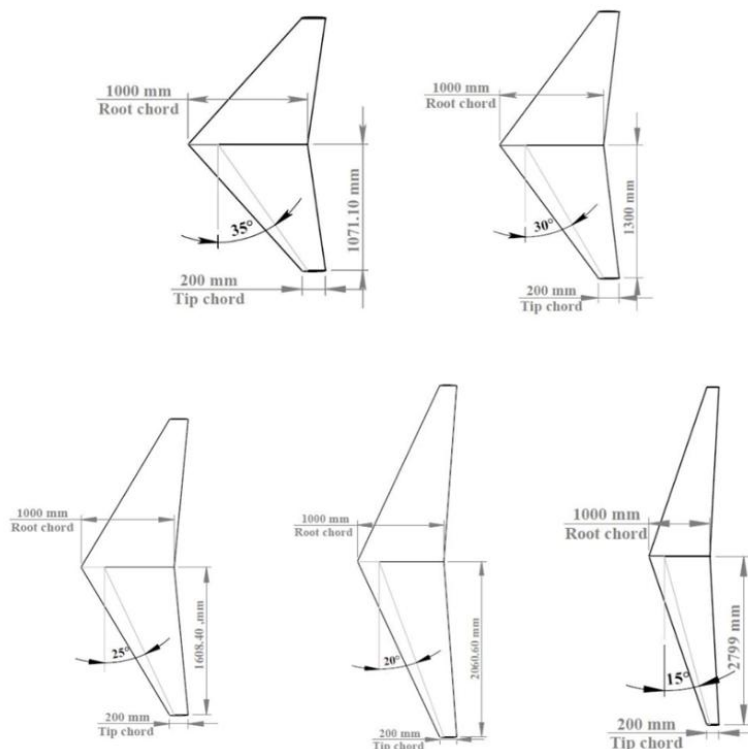


Fig. 6. Shapes and dimension of the five UAV used

5. Mesh Information's. Different angle combinations based on the angle of attack (0° , 2° , and 4°) were used to explore the variations in performance of different sweepback wing angles. The wing model is meshed using the tetrahedron meshing method in all of the simulations presented here. This method was chosen because it was able to capture near-wing complexity while also generating a very fine grid at the boundary layer. In most circumstances, the mesh resolution has a considerable influence on the quality of CFD simulations. The mesh resolution is determined by the number of cells in the computational domain. Increasing the mesh density has minimal influence on the output after a certain point. Mesh reports vary depending on the wing model; Table 1 illustrates a mesh report for a variety of models. Fig. 7 shows a wing mesh with various perspectives. The velocity inlet boundary condition is the intake boundary condition, whereas the pressure outlet boundary condition is the exit boundary condition.

Table 1

Mesh report for a variety of models

Domain / Box	Nodes	Elements
sweepback wing angle 15° , Angle of attack 2°	232371	1311394
sweepback wing angle 20° , Angle of attack 0°	214475	1209814
sweepback wing angle 25° , Angle of attack 4°	201947	1138868
sweepback wing angle 30° , Angle of attack -2°	189816	1069668
sweepback wing angle 35° , Angle of attack 0°	175559	987972

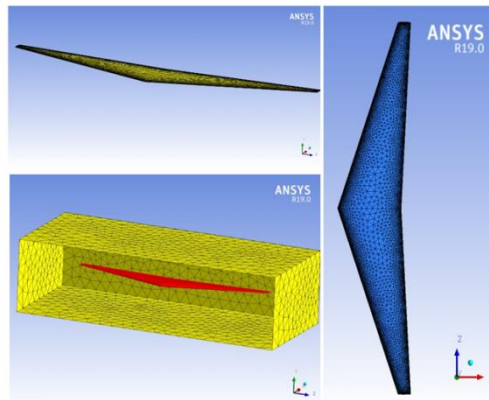


Fig. 7. Wing mesh with various viewpoints

6. Calculation and Results. 6.1. Calculated the aspect ratio. To calculate the AR, first wing area must be calculated, Wing area,

$$A = 0.5 * (C_r + C_t) * s.$$

Knowing $C_r = 1000 \text{ mm}$, $C_t = 200 \text{ mm}$

s : semi-span, $s = \frac{b}{2}$, is changing to each UAV model, $b = \text{Wing span}$.

For UAV with sweep angle = 35°, s = 1071.1 mm,
 sweep angle = 30°, s = 1300 mm,
 sweep angle = 25°, s = 1608.4 mm,
 sweep angle = 20°, s = 2060.6 mm,
 sweep angle = 15°, s = 2799 mm,

$A_{35} = 642660 \text{ mm}^2$
 $A_{30} = 780000 \text{ mm}^2$
 $A_{25} = 965040 \text{ mm}^2$
 $A_{20} = 1236360 \text{ mm}^2$
 $A_{15} = 1679400 \text{ mm}^2$

Aspect ratio, $AR = \frac{b^2}{A}$ or $\frac{b}{c}$

A = Wing area, c = chord, b = Wing span

$AR_{35} = 7.14$.

$AR_{30} = 8.66$.

$AR_{25} = 10.72$.

$AR_{20} = 13.74$.

$AR_{15} = 18.66$.

The results can see it in Fig. 8.

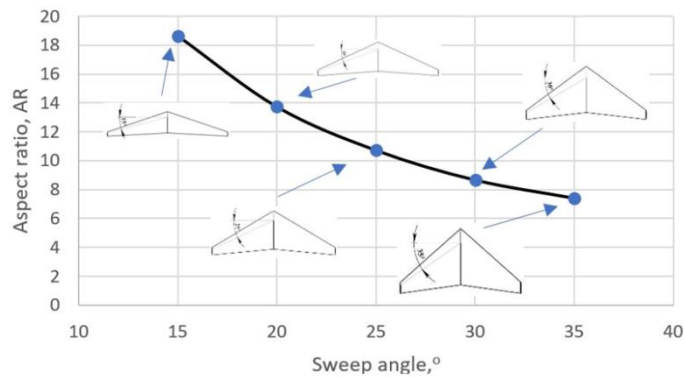


Fig. 8. Aspect ratio versus swept-back wing

6.2. Lift, drag, and Lift to drag ratio Calculations. A CFD Fluent (ANSYS) software simulation to five UAV models have been done, each model tested with three angles of attack (0°, 2°, and 4°). firstly, force of lift value calculated. The results in Fig. 9 show all models are close to each other at angle of attack 0° then the models start to differ in values gradually through angle of attach 2° until to reach maximum difference at angle of attack 4°. The most important thing to notice that the best results of lift force have lower sweepback angle as fallow (S refer to sweep-back angle), $S_{15} = 312$, $S_{20} = 210$, $S_{25} = 150$, $S_{30} = 109$, and $S_{35} = 81$ and all values at angle of attack equal to $AOA = 4^\circ$.

Secondly, the results of drag force shown in Fig. 10, the differ between the of value of drag force of models can be seen from angle of attack 0° and gradually increase with the increasing of angle of attack and also the best results of lift force have lower sweep-back angle as fallow $S_{15} = 7.5$, $S_{20} = 5.4$, $S_{25} = 4.1$, $S_{30} = 3.3$, and $S_{35} = 2.6$ and all values at angle of attack equal to $AOA = 4^\circ$.

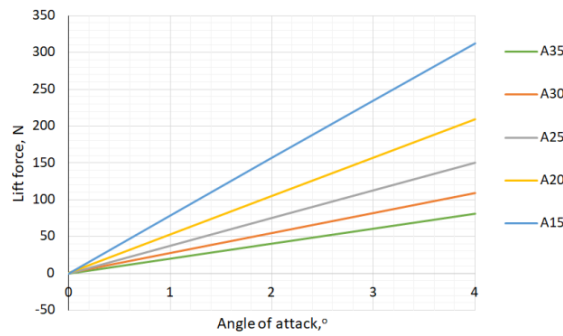


Fig. 9. The lift force versus the angle of attack

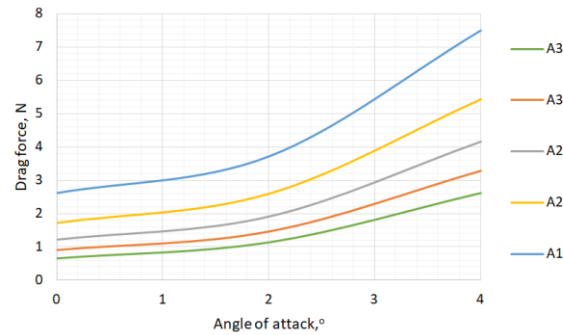


Fig. 10. The drag force versus the angle of attack

After calculation lift and drag force, the results are logical but it not gives us a good indication which model has better result because of the model not only must has high lift force but also lower drag force and lift to drag ratio gives us such indication. In Fig. 11, the results show that the values have almost same results at angle of attack equal to 0° and start to rises until it reaches angle of attack equal to 2° which is the best results, then the values of lift to drag minimize. Best results occur at low sweepback angle as fallow $S_{15} = 42$, $S_{20} = 40.5$, $S_{25} = 39.6$, $S_{30} = 37$, and $S_{35} = 35.5$ and all values at angle of attack equal to $AOA = 2^\circ$.

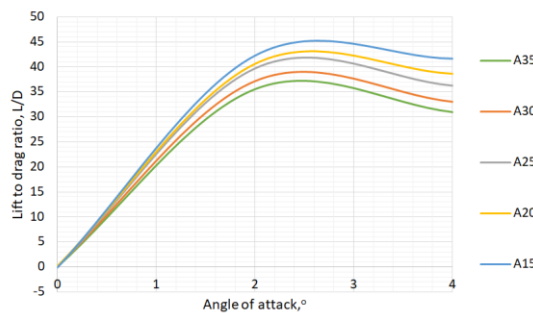


Fig. 11. Lift to drag ratio versus the angle of attack

6.3. CFD simulation analysis. In Fig. 12, the CFD simulation analysis for the UAV by the FLUENT ANSYS software for the two models (maximum value lift to drag ratio model UAV with $S_{15} A_2$ and minimum value lift to drag ratio model UAV with $S_{35} A_0$) for pressure counter, A & B for root chord, C for tip chord and the different of pressure distribution can be noticed for two models. In Fig. 9, case of maximum value of lift to drag ratio, the CFD photo show the pressure on the top of the wing is less than the pressure on the bottom of the wing. The difference in pressure creates a force on the wing that lifts the wing up into the air. And on the contrary, case of minimum value of the lift to drag ratio the pressure distribution over the wing is almost identical which cause minimum lift force.

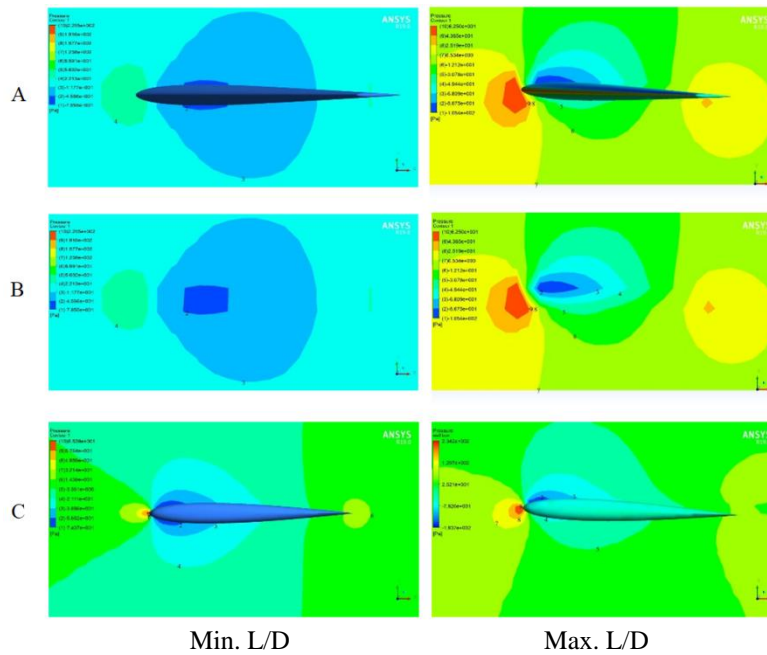


Fig. 12. Pressure contours for two UAV one with maximum lift to drag ratio and another with minimum lift to drag ratio

Conclusions. Unmanned Aerial Vehicles (UAVs) are now widely employed in practically every industry, ranging from military to commercial. The creation of an unmanned aerial vehicle is in great demand. Because it's difficult to interpret UAV's conceptual design data due to a lack of data sheets, CFD is utilized instead. Due to considerable improvements in computers, Computational Fluid Dynamics (CFD) has become the most preferred approach for designers to obtain the component of the aircraft by completing the required aerodynamic form using fluid dynamics and pressure distribution. CFD gives precise predictions of the wing's aerodynamic properties, allowing them to be modified and optimized for the best outcomes. When viewed from above, the form of a wing is known as the shape of the wing. The induced drag coefficient and stalling characteristics are the key aerodynamic parameters impacted by shape, which are directly connected to the aspect ratio and taper. The wing's size and form, the angle at which it meets approaching air, the speed at which it passes through the air, and even the density of the air all have an impact on lift. In this paper, UAV designed with different sweep-back angle (15° , 20° , 25° , 30° , and 35°), SD8020 airfoil used for root chord = 1000 mm,

and tip chord = 200 mm, and different aspect ratio with constant taper ratio = 0.2, all models examine versus the attack angle (0° , 2° , and 4°), the results show that the lift to drag ratio (aerodynamics efficiency) increase by increasing the aspect ratio and increasing the sweepback angle. best results with maximum lift to drag ratio in UAV model with sweepback angle 15° at angle of attack = 2° with aspect ratio 18.66, lower lift to drag ratio occur in UAV model with sweepback angle 35° at angle of attack = 0° with aspect ratio 7.14.

REFERENCES

1. *Gudmundsson S.* General aviation aircraft design: Applied Methods and Procedures. Butterworth-Heinemann, 2013.
2. *Bakar A., Ke L., Liu H., Xu Z., and Wen D.* Design of low altitude long endurance solar-powered UAV using genetic algorithm, *Aerospace*, 2021, 8, (8), pp. 228.
3. *Ruzgienė B., Aksamitauskas Č., Daugėla I., Prokopimas Š., Puodžiukas V., and Rekus D.* UAV photogrammetry for road surface modelling, *Baltic journal of road and bridge engineering*, 2015, 10, (2), pp. 151-158.
4. *Marqués P.* Advanced UAV aerodynamics, flight stability and control: an Introduction, *Advanced UAV aerodynamics, flight stability and control: novel concepts, theory and applications*, 2017, pp. 1.
5. *Chung P.-H., Ma D.-M., and Shiau J.-K.* Design, manufacturing, and flight testing of an experimental flying wing UAV, *Applied Sciences*, 2019, 9, (15), pp. 3043.
6. *Himer S.E., Ouaisa M., Ouaisa M., and Boulouard Z.* General Parametric of Two Micro-Concentrator Photovoltaic Systems for Drone Application, *Computational Intelligence for Unmanned Aerial Vehicles Communication Networks*. Springer, 2022, pp. 275-289.
7. *Al-Turjman F.* Unmanned Aerial Vehicles in Smart Cities. Springer, 2020.
8. *Bertin J.J., and Cummings R.M.* Aerodynamics for engineers. Cambridge University Press, 2021.
9. *Houghton E.L., and Carpenter P.W.* Aerodynamics for engineering students. Elsevier, 2003.
10. *Hitchens F.* The encyclopedia of aerodynamics. Andrews UK Limited, 2015.
11. *Sóbester A., and Forrester A.I.* Aircraft aerodynamic design: geometry and optimization. John Wiley & Sons, 2014.
12. *Anderson J.* EBOOK: Fundamentals of Aerodynamics (SI units). McGraw hill, 2011.
13. *Fahlstrom P.G., Gleason T.J., and Sadraey M.H.* Introduction to UAV systems. John Wiley & Sons, 2022.
14. *Collicott S.H., Valentine D.T., Houghton E., and Carpenter P.* Aerodynamics for Engineering Students. Butterworth-Heinemann, 2016.
15. *Gülçat Ü.* Fundamentals of modern unsteady aerodynamics. Springer, 2010.
16. *Dragos L.* Mathematical methods in aerodynamics. Springer Science & Business Media, 2003.
17. *Nguyen M.T., Nguyen N.V., and Pham M.T.* Aerodynamic analysis of aircraft wing, *VNU Journal of Science: Mathematics-Physics*, 2015, 31, (2).
18. *Küchemann D.* 'he aerodynamic design of aircraft' (American Institute of Aeronautics and Astronautics, Inc., 2012).
19. *Moran J.* An introduction to theoretical and computational aerodynamics. Courier Corporation, 2003.
20. *Anderson D.F., and Eberhardt S.* Understanding flight. McGraw-Hill Education, 2010.

Статью рекомендовал к опубликованию д.т.н., профессор В.В. Курейчик.

Аль-Хафаджи Али Дж. Давуд – Технологический университет; e-mail: alhafadzhi@sfedu.ru, ali.j.dawood@uotechnology.edu.iq; г. Багдад, Ирак; тел.: +79851677562, +9647724255278; преподаватель; канд. наук; аспирант ЮФУ.

Панатов Геннадий Сергеевич – Южный федеральный университет; e-mail: gspanatov@sfedu.ru; г. Таганрог, Россия; кафедра летательных аппаратов; д.т.н.; профессор.

Болдырев Антон Сергеевич – e-mail: boldyrev@sfedu.ru; тел.: 89888987877; директор Института радиотехнических систем и управления ЮФУ; к.ф.-м.н.; доцент.

Al-Khafaji Ali J. Dawood – University of Technology; e-mail: alhafadzi@sfedu.ru, ali.j.dawood@uotechnology.edu.iq; Baghdad, Iraq; phones: +79851677562, +9647724255278; lecturer; graduate student at Southern Federal University.

Panatov Gennadiy Sergeevich – Southern Federal University; e-mail: gspanatov@sfedu.ru; Taganrog, Russia; aircraft department; dr. of. eng. sc.; professor.

Boldyrev Anton Sergeevich – e-mail: boldyrev@sfedu.ru; phone: +79888987877; director of the Institute of Radio Engineering Systems and Control of the Southern Federal University; cand. of phys. and math. sc.; associate professor.